NASA Technical Memorandum 87100

Microstructures in Rapidly Solidified Ni-Mo Alloys

N. Jayaraman
University of Cincinnati
Cincinnati, Ohio

and

S.N. Tewari, K.J. Hemker, and T.K. Glasgow
Lewis Research Center
Cleveland, Ohio

Prepared for the
International Conference on Rapidly Solidified Materials
sponsored by the American Society for Metals
San Diego, California, February 3-5, 1985

NASA

ABSTRACT

Ni-Mo alloys of compositions ranging from pure Ni to Ni-40 at % Mo were rapidly solidified by Chill Block Melt Spinning in vacuum and were examined by optical metallography, x-ray diffraction and transmission electron microscopy. Rapid solidification resulted in an extension of molybdenum solubility in nickel from 28 to 37.5 at %. A number of different phases and microstructures were seen at different depths (solidification conditions) from the quenched surface of the melt spun ribbons.

RAPIDLY SOLIDIFIED ALLOYS exhibit greatly refined microstructure, extended solid solubility, and metastable phase formation. The microstructures produced in these materials depend on alloy composition and local solidification parameters. In this paper the microstructural features observed in binary nickel-molybdenum alloys after Chill Block Melt Spinning are presented. This study forms the basis for investigation of other more complex Nickel-base alloy systems.

The equilibrium phase diagram for the Ni-Mo eutectic system (Ref. 1) is shown in Fig. 1. Under equilibrium the maximum solid solubility of Mo in Ni is 28.4 at %. ß-phase (NiMo) has an equilibrium composition range from 51 to 53 at % Mo. The goal of this study was to decermine the effect of rapid solidification on the microstructures of Ni-Mo alloys.

EXPERIMENTAL

The Ni-Mo ribbons used in this study were cast on a 4340 steel wheel by the free jet Chill Block Melt Spinning (CBMS) process at the NASA-Lewis Research Center. This facility is described in Ref. 2. Ni-Mo alloys of the compositions, Ni-0, 5, 17.5, 21, 27.5, 35, 37.5 and 40 at % Mo were used.

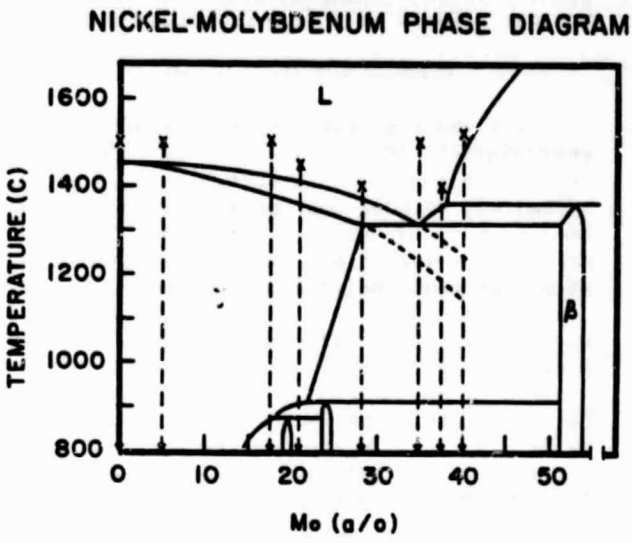

Figure 1. - Nickel-Molybdenum phase diagram. X's indicate casting temperatures and compositions.

All ribbons were examined by x-ray diffraction using Cu-Kα radiation on both sides (wheel and free) of the ribbons. In this paper the quenched side of the ribbon will be referred to as the wheel side, and the side away from the wheel will be referred to as the free side. Cross sections of the samples etched with Marble's Reagent were examined by optical metallography. Transmission electron microscopy (TEM) was carried out for three alloys, namely Ni-27.5 at % Mo (hypoeutectic), Ni-35 at % Mo (eutectic) and 37.5 at % Mo (hypereutectic). Three regions of the melt-spun ribbons, namely wheel side, midsection and the free side were examined. Of these three sections the wheel side represents the fastest quench region. Samples were electropolished by a twin jet method using an ethanol (45 vol %), butyl cellusolve (45 vol %) and perchloric acid (10 vol %) electrolyte cooled to about 0 °C. For examination of

near-wheel and near-free sides, these surfaces were protected by lacquer and the ribbon was thinned only from the other side.

RESULTS AND DISCUSSIONS

Ribbons cast for this search were approximately 40 μm thick, 2.5 mm wide and up to 15 m in length. The castability of pure nickel was so poor that no single layer ribbons of pure nickel were obtained. In general ribbon length and castability increased with increasing molybdenum content.

X-RAY DIFFRACTION - The Ni-fcc phase (γ) was identified in all compositions. The lattice parameter of this phase increased with increasing Mo content up to about 37.5 at % Mo. The lattice parameter data for the rapidly solidified ribbons are compared to conventionally cast samples in Fig. 2. For the conventionally cast material a linear

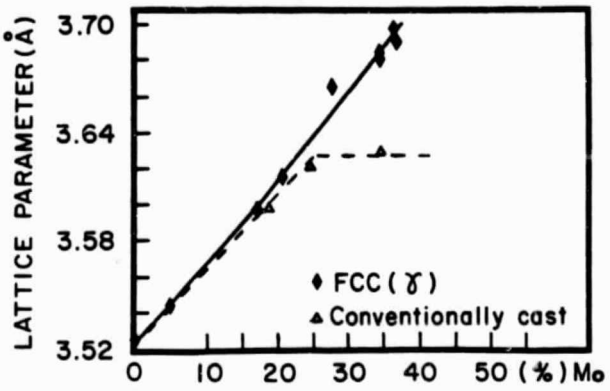

Figure 2. - Lattice parameter of γ as a function of composition for conventionally cast and rapidly solidified alloys.

increase in lattice parameter with the increasing molybdenum content is observed up to about 27.5 at % Mo. The lattice parameter remains constant beyond this molybdenum content, as would be expected from the Ni-Mo phase diagram, Fig. 1.

The extended solid solubility of the rapidly solidified ribbons up to about 37.5 at % Mo is illustrated by the extended straight line relationship between lattice parameter and molybdenum content of the γ phase in this figure. The lattice parameter data in this figure compare well with the values reported for Ni-Mo alloys of the composition 0 to 20 at % Mo (Refs. 3 and 4). This observation of extended solid solubility by rapid solidification is further augmented through TEM analysis. In addition to the extended solid solubility of fcc Ni-phase (γ), indications of ß-NiMo (orthorhombic) were found near the wheel side of ribbons from Ni-35 at % Mo and Ni-37.5 at % Mo alloys. These observations were also found to be consistent with the TEM analysis, as will be shown in a latter section.

OPTICAL METALLOGRAPHY - Metallographic analyses showed the following results: Multiple layer pure Ni ribbons showed very large grains. Alloys of 5 to 28 at % Mo, those in the γ solubility range (Fig. 3), showed cellular/dendritic growth throughout the thickness of the ribbon. The γ grain size was observed to decrease with increasing molybdenum content. Three zones were observed in alloys of higher Mo, >28 at %, content. A featureless zone appeared closest to the wheel (Figs. 3 (d) to (f)). Directly adjacent and separated by a boundary was a planar from growth zone. As the planar front zone broke down, cellular/dendritic grains formed. The amount of the featureless zone increased with increasing Mo content.

TRANSMISSION ELECTRON MICROSCOPY - The results of the TEM analysis of the three alloys studied in detail are summarized in Table I. Figures 4 to 9 show the corresponding typical microstructures. All three alloys showed significant effects of rapid quenching. One of the unique microstructural features was that of supersaturated and faulted Ni-fcc (γ) grains. This was the only microstructure found in the hypoeutectic alloy (27.5 at % Mo) in the near wheel region. Here, as shown in Fig. 4, supersaturated γ-fcc grains were found to nucleate along a line (presumably grinding marks on the quenching wheel) and grow parallel to the wheel surface (region A in Fig. 4). In addition, in several locations, Ni grains appear to have nucleated at a point on the wheel surface and grown radially, (region B in Fig. 4) normal to the wheel surface resulting in grain structures like flower petals. On closer examination of the individual γ grains it was found that most of the grains contained finely spaced linear features (Fig. 5). These features are due to planar faults, which could be considered as microtwinned platelets of about 15 Å thickness. Detailed diffraction analysis of these are described elsewhere (Ref. 5). These faulted γ grains were also found in the eutectic alloy (35 at % Mo) near the wheel-side and in the hypereutectic alloy (37.5 at % Mo) in the mid section. Figure 5 is typical of the faulted γ grains found in the alloys.

The eutectic and hypereutectic alloys showed a fine NiMo microscrystalline region near the wheel side of the ribbon (Fig. 6). This is believed to have formed by crystallization of an amorphous phase which initially formed during quenching. The hypereutectic alloy showed an amorphous region surrounded by ß-NiMo grains (Fig. 7). In-situ heating of the amorphous regions in the TEM produced a distribution of fine microcrystallites similar to the ones shown in Fig. 6.

(c) 28%

(f) 40%

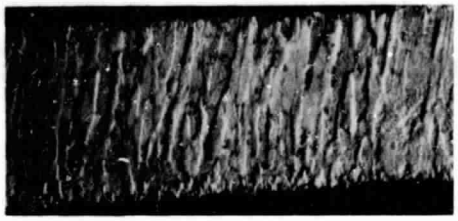

(b) 17.5%

(e) 37%

(a) 5%

Wheel side

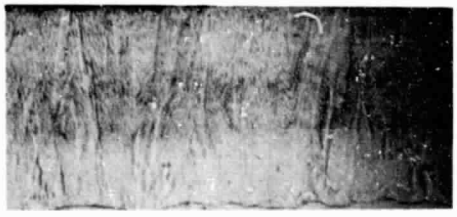

(d) 35%

Wheel side

Figure 3. - Thru thickness microstructures of ribbons for Ni-5, 17.5, 28, 35, 37 and 40 at % Mo alloys.

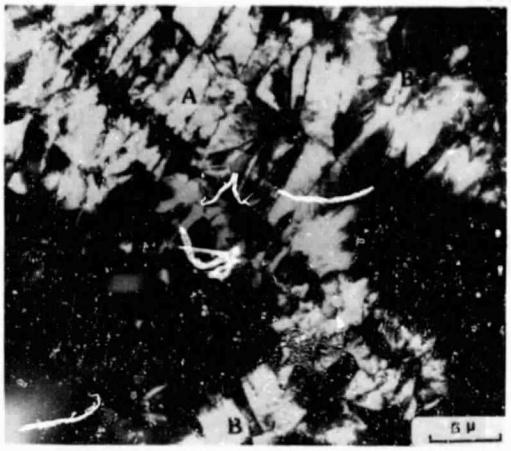

Figure 4. - Bright field TEM micrograph showing γ-Ni (fcc) grains in hypoeutectic alloy in the near wheel side region of the ribbon.

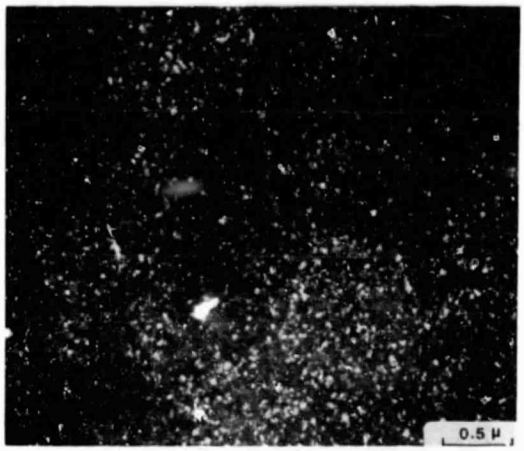

Figure 6. - Typical microcrystalline ß-NiMo regions seen in eutectic (near wheel side) and hypereutectic (near wheel side) alloy ribbons.

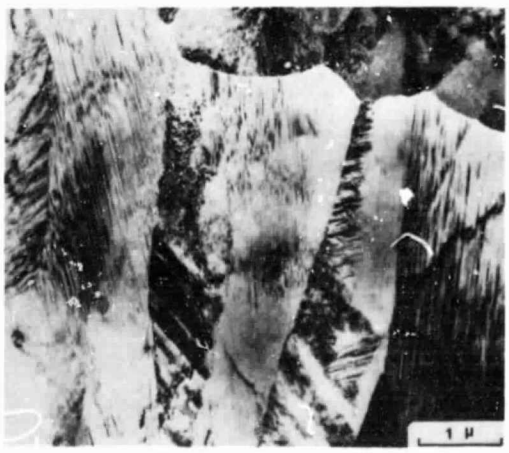

Figure 5. - Typical faulted γ-fcc Ni grains in hypoeutectic (near-wheel side), eutectic (near-wheel side) and hypereutectic (midsection) alloy ribbons.

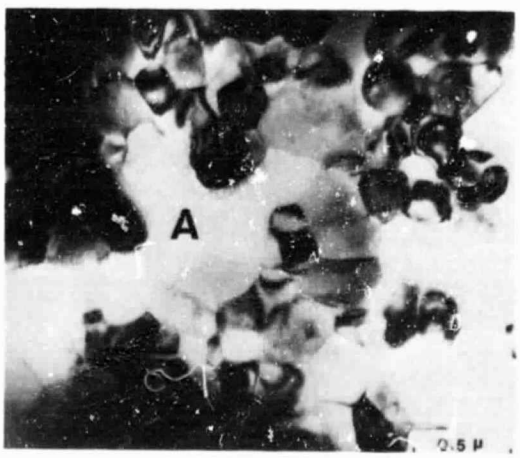

Figure 7. - Amorphous phase (region A) surrounded by ß-NiMo grains in the hypereutectic alloy ribbon (near wheel side).

Another unique microstructure is the faulted ß-NiMo grains found in the mid-sections of hypereutectic (37.5 at % Mo) ribbons. The fault contrast is seen both in the bright field and dark field images shown in Fig. 8.

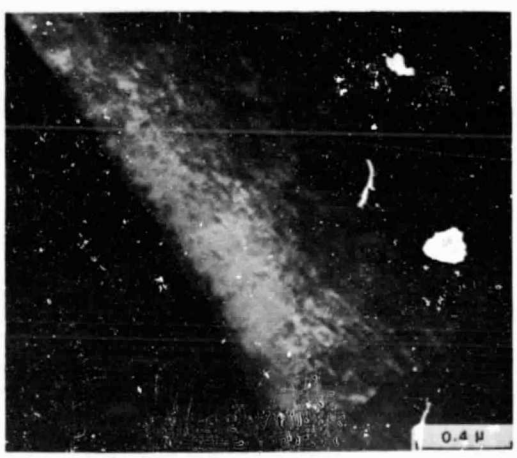

Figure 8. - Bright field (a) and dark field (b) TEM micrographs of ß-NiMo grains (faulted ?) seen in hypereutectic (mid-section) alloy ribbons.

Dendritic γ cells were found in the midsection and free surface region of all three alloys. The typical cellular appearance as shown in Fig. 9 was the same for all three alloys. The fraction of the inter-dendritic eutectic found in the γ dendrites was greater in the near free surface regions than other part of the ribbon. It also increased with the increasing molybdenum content of the alloy.

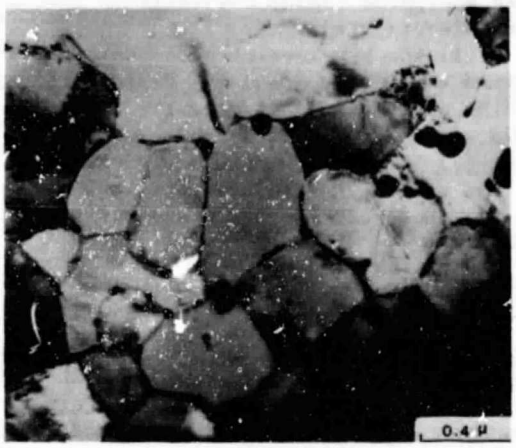

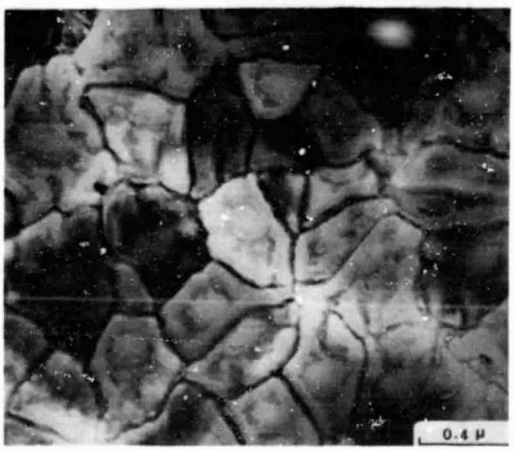

Figure 9. - Typical cellular/dendritic microstructures found in hypoeutectic (midsection and near free surface), eutectic (midsection and near free surface) and hypereutectic (midsection and near free surface). (a) shows a typical cellular structure without any intercellular eutectic and (b) shows a typical dendritic structure with inter-dendritic eutectic.

CONCLUSIONS

The following conclusions were made from this study of rapidly solidified Ni-Mo alloy ribbons:

(1) Molybdenum solid solubility in fcc Ni (γ) was extended from about 28 to 37.5 at % Mo by rapid solidification. It resulted in the formation of γ grains with planar-faults.

(2) Alloys with molybdenum content at and above the eutectic composition (>35 at % Mo) showed an amorphous phase as

a result of rapid solidification. Some of this amorphous region crystallized into very fine microcrystallites.

(3) The hypereutectic composition alloy formed very large, faulted, orthorhombic ß-NiMo grains, even at moderate cooling rates (mid sections of ribbons).

(4) In the slow cooled regions all the alloys showed the cellular/dendritic growth of γ phase with γ/ß interdendritic eutectic.

ACKNOWLEDGMENT

Appreciation is expressed to R.W. Jech, T.J. Moore and N.W. Orth for preparing the melt-spun ribbons. Special thanks are due to Dr. Hugh R. Gray for his keen interest and continuous encouragement.

REFERENCES

1. Metals Handbook, Vol. 8, p. 319, American Society for Metals, Metals Park, OH, 1973.

2. R.W. Jech, T.J. Moore, T.K. Glasgow, and N.W. Orth: J. Met., 1984, Vol. 36, No. 4 pp. 41-45.

3. W.B. Pearson: Handbook of Lattice Spacings and Structures of Metals and Alloys, p. 753, Pergamon Press, New York, 1958.

4. C.R. Brooks, J.E. Spruiell, and E.E. Stansbury: Int. Met. Rev., 1984, Vol. 29, pp. 210-248.

5. N. Jayaraman, and S.N. Tewari: NASA Lewis Research Center, Cleveland, OH, unpublished research, 1985.

TABLE I. - SUMMARY OF PHASES AND MICROSTRUCTURES IN RAPIDLY SOLIDIFIED RIBBONS OF Ni-Mo ALLOYS.

Position of ribbon	Alloy		
	Ni-27.5 at % Mo, hypoeutectic	Ni-35 at % Mo, eutectic	Ni-37.5 at % Mo hypereutectic
Near wheel	Supersaturated faulted γ grains (Figs. 4 and 5)	(1) Faulted γ grains (Fig. 5) (2) Microcrystalline ß, NiMo (Fig. 6)	(1) Amorphous phase (Fig. 7) (2) Microcrystalline ß, NiMo (Fig. 6) (3) Fine ß, NiMo grains (Fig. 7)
Midsection	γ cells/dendrites (Fig. 9(a))	γ cells/dendrites (Fig. 9(a))	(1) Faulted γ grains (Fig. 5) (2) Large ß, NiMo grains (Fig. 8) (3) γ cells (Fig. 9(a))
Free surface	γ dendrites with interdendritic eutectic (Fig. 9(b))	γ dendrites with interdendritic eutectic (Fig. 9(b))	γ dendrites with interdendritic eutectic (Fig. 9(b))

1. Report No.	2. Government Accession No.	3. Recipient's Catalog No.
NASA TM-87100		

4. Title and Subtitle	5. Report Date
Microstructures in Rapidly Solidified Ni-Mo Alloys	505-33-62
	6. Performing Organization Code

7. Author(s)	8. Performing Organization Report No.
N. Jayaraman, S.N. Tewari, K.J. Hemker, and T.K. Glasgow	E-2694
	10. Work Unit No.

9. Performing Organization Name and Address	11. Contract or Grant No.
National Aeronautics and Space Administration Lewis Research Center Cleveland, Ohio 44135	
	13. Type of Report and Period Covered
12. Sponsoring Agency Name and Address	Technical Memorandum
National Aeronautics and Space Administration Washington, D.C. 20546	14. Sponsoring Agency Code

15. Supplementary Notes

N. Jayaraman, University of Cincinnati, Dept. of Metallurgical Engineering, Cincinnati, Ohio 45221-0012, S.N. Tewari, NRC-NASA Research Associate, on leave from Defense Metallurgical Research Laboratory, Hydorabad, India; K.J. Hemker and T.K. Glasgow, NASA Lewis Research Center. Prepared for the International Conference on Rapidly Solidified Materials, sponsored by the American Society for Metals, San Diego, California, February 3-5, 1985.

16. Abstract

Ni-Mo alloys of compositions ranging from pure Ni to Ni-40 at % Mo were rapidly solidified by Chill Block Melt Spinning in vacuum and were examined by optical metallography, x-ray diffraction and transmission electron microscopy. Rapid solidification resulted in an extension of molybdenum solubility in nickel from 28 to 37.5 at %. A number of different phases and microstructures were seen at different depths (solidification conditions) from the quenched surface of the melt spun ribbons.

17. Key Words (Suggested by Author(s))	18. Distribution Statement
Rapid quenching; undercooling; Melt spinning	Unclassified - unlimited STAR Category 26

19. Security Classif. (of this report)	20. Security Classif. (of this page)	21. No. of pages	22. Price*
Unclassified	Unclassified		